

Circumstellar masers

J. Alcolea

Observatorio Astronómico Nacional (OAN-IGN), C/ Alfonso XII Nº 3 y 5, E-28014 Madrid, Spain

Abstract. Circumstellar masers are unique tools for probing the envelopes around low mass dying stars using VLBI. In this contribution I briefly review the status of our knowledge on these emissions, especially focusing on the latest results obtained by means of VLBI observations. I also outline some of the new windows that will open for VLBI maser research thanks to the upcoming new instrumentation.

1. Introduction

Stars are tiny. In fact they are about the tiniest things one can find among astrophysical objects. The bigger a star can get is of the order of several AU in the case of red super-giants, but (obviously) this size is just about 1'' at a distance of 1 pc, and only 1 m.a.s. at a more typical distance of 1 kpc. From this simple reasoning, it is easy to see why the study of stars benefits from the use of the VLBI technique, which provides spatial resolutions of a fraction of a m.a.s. at the highest available frequencies.

However, the observation of stars using VLBI is not so straight forward. VLBI provides very high angular resolution but we have to pay a price for it: we can only observe sources that at the same time are very compact and very bright. With the current instrumentation, VLBI flux sensitivities and resolving power imply lower detection limits for the brightness temperature from tens to hundreds of thousand degrees, in the case of continuum observations. The situation is of course much more restrictive for spectral line studies, where minimum brightness temperatures much higher are required. For example, for a spectral resolution of a fraction of km s^{-1} , the VLBA sensitivity at 7 and 3 mm is about several 10^8 K . In practice, these limits exclude the detection of *almost* any radiation of thermal origin, and typically VLBI studies deal with non-thermal sources: synchrotron and gyro-synchrotron emission in continuum studies, and maser emission and absorption in front of very strong non-thermal radio-continuum sources, in the case of spectral line works. However, I recall that behind these restrictions on minimum brightness temperature, there is no instrumental limitation other than sensitivity, and that relaxing those limits is just a matter of having more collecting area, better receivers, and, for the case of the continuum, broader simultaneous passbands.

In any case, the current VLBI sensitivity restricts the number of stellar sources and/or processes that can be observed. In particular, we can hardly speak of detecting the stars themselves, only in the case of strong radio stars, but rather their ejecta and surrounding environments. In particular, VLBI studies of stars and related sources (proto-stars and star forming regions, and stellar ashes) include the observation of stellar magneto-spheres (M dwarfs, T Tauris, pulsars), of the high-speed ejecta of very compact sources (black holes, neutron

stars, white dwarfs), and the maser emission from several molecular species.

Maser emission occurs when there is an inversion in the populations of the two levels of one transition (i.e. the upper level is more populated than the lower level), leading to an exponential amplification of the radiation that can attain extremely high brightness temperatures. These inversions are induced by asymmetries in the population/de-population processes of the energy levels connected by the maser transitions. (For example, in H_2O masers the upper levels of the transitions are mainly populated via collisions, while the de-excitation is due to radiative decays.) The maser emission itself tends to destroy the inversion, therefore, for the maser to maintain its power, a strong source of energy is required. This is the reason why masers are always associated to very luminous and energetic sources, AGNs, SNRs, high-mass proto-stars and Asymptotic Giant Branch stars. In the following sections I will give a general background on this last type of masers, also known as circumstellar masers, since they arise in the molecular envelopes around these stars. I will also highlight some of the latest results that have been obtained by VLBI observations of these strong emissions, focusing on their impact on aspects such as the maser pumping theory, the structure, dynamics and evolution of these envelopes, Astrometry and distance estimation, etc. Finally, I will outline how circumstellar maser studies may benefit from using the new and improved VLBI instrumentation, also in combination with other techniques, that is becoming or will become available within the next coming years.

2. Circumstellar envelopes

Stars with initial masses between 1 and $8 M_\odot$ end their lives rather quietly, but also throwing away a large portion of the stuff they are made of. These mass losses occur mainly at the end of their evolution, while in the Asymptotic Giant Branch (AGB) phase, and more specifically at the very end of it. Due to their moderate initial mass, after the Hydrogen and the Helium have been exhausted at the center of these stars, the core degenerates and the atomic reactions do not proceed in it any further. The energy of the star is mainly due to the CNO cycle occurring in layers outside the nucleus, which are surrounded by a deep convective mantle. The star becomes very luminous,

10^4 to $10^5 L_\odot$, but at the same time very big, larger than 1 AU, resulting in a red giant/super-giant, i.e. an AGB star.

While in the AGB, stars are radial pulsators. These pulsations occur in periods of one to two years, resulting in changes in the size (as large as 50%) and temperature of the star. This is the reason why these objects are also known as Long Period Variables (LPVs). According to their brightness and regularity of their variation, LPVs are divided in Miras (regular giants), semi-regulars (semi-regular giants) and super-giants.

During these pulsations, the atmosphere of the star rises and sinks at speeds of tens of km s^{-1} . These velocities are of the order of the escape velocity, and hence the material of the upper layers of the star is very weakly attached to it. The shock waves produced by the periodic pulsation form an extended atmosphere up to several stellar radii, where the density is still high but the temperature is below the condensation point for dust grains to form. Once dust grains are formed, they are kicked away by the impacts of the stellar photons. As the dust grains move out, they collide with the gas molecules and both gas and dust start a radial expansion thanks to the *radiation pressure* (provided that it can overtake the gravitational force). After a period of acceleration, and since both stellar radiation and gravity rapidly decrease as $1/r^2$, the material expands freely, forming a spherically symmetric envelope moving at a constant velocity of 10 to 30 km s^{-1} . This process results in a mass loss that at the end of the AGB can attain rates as high as $10^{-4} M_\odot \text{ yr}^{-1}$, and that will determine the future evolution of both the star and the envelope. See Olofsson (1999) for a short review on AGB stars.

These circumstellar envelopes (CEs) are of course rich in dust and molecules, that can be observed mostly by means of the IR continuum emission (dust), and many spectral lines at cm, mm and sub-mm wavelengths (molecules). The chemical composition of the envelope strongly depends on the composition of the central star. According to their elementary abundances, AGB stars can be divided in O-rich, with $[\text{O}]/[\text{C}] > 1$, and C-rich, where $[\text{O}]/[\text{C}] < 1$. There is also a minor type in between, named S-type, for which $[\text{O}]/[\text{C}] \approx 1$. In addition, one of the most stable molecules in CEs is the carbon monoxide, CO. For O-rich stars we can assume that CO forms until Carbon is exhausted in the gas phase. This is the reason why O-rich envelopes are poor in C-bearing molecules other than CO, and their dust grains mainly consist of silicates. On the contrary, C-rich envelopes present lower abundances of O-bearing molecules, apart from CO, than O-rich sources, and so their dust grains are formed of carbonaceous compounds. See Habing (1996) for a very complete review on both AGB stars and their CEs.

3. Circumstellar masers

Luckily, some of these circumstellar spectral lines are masers, allowing their study using VLBI. So far 5 molecular species have been found to be masering in circumstellar envelopes: OH, H_2O and SiO in envelopes of O-rich sources, and SiS and HCN in envelopes of C-rich sources. Very little is known on the masers of the C-rich stars, mostly based on single dish observations. They are detected just in a handful of sources, and

to date no successful VLBI observations of these masers have been reported. SiS shows maser emission in the $J=1-0$ line in the prototype source IRC +10216 (CW Leo). The line profile is U-shaped, the blue-shifted component being more intense than the red-shifted one, see Nguyen-Q-Rieu et al. (1984). This could be a case similar to the OH masers, including some amplification of the stellar continuum on the blue peak (see Sect. 3.1). HCN masers are detected in the $J=1-0$ transition of the ground state (Izumiura et al. 1995) at 89 GHz, and in three rotational lines of vibrationally excited states: the $J=1-0$ line of the (02^00) state (Lucas et al. 1988), the $J=2-1$ line of the $(01^{1c}0)$ state at 178 GHz (Lucas & Cernicharo 1989), and the $J=9-8$ line of the (04^00) state at 805 GHz (Schilke et al. 2000). More recently, Schilke & Menten (2003) have discovered maser/laser emission from the (ro-vibrational) cross-ladder $(11^10)-(04^00)$ $J=10-9$ transition at 891 GHz.

Contrary to what happens in C-rich envelopes, masers in O-rich stars are very widespread. They are detected in hundreds of sources and very complete statistical studies exist. In addition, there are also many high spatial resolution observations, either with VLBI or connected interferometry. Another important aspect of the three species found to be masering in O-rich envelopes, OH, H_2O and SiO, is that they are somehow quite complementary, since each of them arises from the one of the three major parts we can distinguish in these envelopes: the pulsating environment near the star (SiO masers), the regions where the envelope is being accelerated by the impact of the photons onto the grains (H_2O masers), and the outer envelope characterized by a constant expansion velocity (OH masers). This certainly provides a very complete view of the envelope just from the observations of these three types of masers.

3.1. High precision Astrometry using OH masers

OH maser emission in CEs occurs in three different transitions at 18 cm: the two main lines at 1665 and 1667 MHz, and the satellite lines at 1612 MHz, between levels in the ground $^2\pi_{3/2}$ $J=3/2$ state. In all cases, these OH masers are pumped via $^2\pi_{3/2}-^2\pi_{1/2}$ $J=3/2-5/2$ transitions at $35 \mu\text{m}$, which absorb the radiation emitted by the circumstellar dust. OH masers are detected in the outskirts of the circumstellar envelope, at distances from the star of the order of 10^{16} cm . This location is due to the fact that OH is a very reactive radical and can only survive for some time in low density regions. In fact for OH to appear in the envelope, we need first to photo-dissociate the parent molecule, H_2O . Since the central star is cool, the photons required to break H_2O are provided by the interstellar UV radiation field. These photons efficiently penetrate in the outer layers of the envelope, where the dust density is low enough so not to block them. Of course the UV radiation also destroys the OH radical, and so the masers are confined to the layers between those of the photo-destruction of H_2O and OH itself. Main lines are dominant in stars with low mass loss rates. As the envelope becomes thicker, 1612 MHz masers take over, but for very thick envelopes the 1667 MHz line becomes dominant again. The line profiles of the OH masers are very characteristic: they are U-shaped. This profile is simply because OH

masers arise from a thin shell that is radially expanding at an almost constant velocity (of some tens of km s^{-1} , much larger than the turbulence velocity of the gas). Because of this particular velocity field and geometry, for any observer, the light trajectories for which the velocity coherence path (and maser amplification) is the largest, are those passing near the star, i.e. both most blue-shifted and red-shifted ones. This model was confirmed with the first observations of OH masers using MERLIN (Booth et al. 1981) and the VLA (Baud 1981).

Since the masers are pumped via the IR radiation of the star, the OH masers also vary with the same period (Herman & Habing 1985). A delay is observed between the maxima for the blue and red peaks, simply due to the extra path that the light coming from the receding part of the envelope needs to travel. In fact, this delay can be used to measure the diameter of the emitting shell d , which is given by $d = ct$, where c is the speed of light, and t is the measured delay of the red-shifted peak w.r.t. the blue-shifted one (Jewell et al. 1980). In addition, the diameter of the shell in the plane of the sky measured in angular units θ , is just the diameter of the emission at the systemic velocity (at the mid point between the two peaks). Assuming that the shell is spherically symmetric, we obtain that the distance to the star D , is given by $\theta = d/D$ (see Spaans & van Langevelde 1992 for further details).

OH maser emission is too big in stars for deserving VLBI observation just from cartographic consideration. In fact, most of the emission is resolved out when observed with long baseline interferometry. However, the VLBI observation of this emission has a potential impact in Astrometry studies as Vlemmings et al. (2003) have recently shown. Following the model described before, it is clear that the most blue-shifted emission should correspond to the line of sight passing through the star. It is then possible that this blue peak would be also amplifying the continuum of the star itself. If this is the case, the astrometric measurement of such a spot would directly give us the accurate position of the star behind. Repeating this measurement for a period of several years, we will obtain the proper motion of the star superimposed on the movement due to the annual parallax. Provided that we can separate both effects on the measured trajectory of the star/maser spot on the sky, we will directly obtain the distance to the target. This technique has been used by Vlemmings et al. in two sources, U Her and W Hya, obtaining results in agreement with Hipparcos distances. In two more cases, R Cas and S CrB, they used a compact red spot, hoping that its relative motion w.r.t. the star is small. In these cases the obtained distances were almost consistent with Hipparcos data.

3.2. Measuring the acceleration of the envelope using water vapor masers

Moving inwards to denser regions in the envelope, the next maser region we find is that of the 22 GHz H_2O masers, corresponding to the $6_{1,6}-5_{2,3}$ rotational transition in the ground vibrational state. The 22 GHz line is not the only transition of H_2O showing maser action, but it is certainly the best studied and observed among water masers, and the only one for which

high spatial resolution images are available. For the other maser lines very little is known. In addition to the 22 GHz line, there are circumstellar water masers detected in the $3_{1,3}-2_{2,0}$ (183 GHz), $10_{2,9}-9_{3,6}$ (231 GHz), and $5_{1,5}-4_{2,2}$ (325 GHz) lines from the ground vibrational state (see Cernicharo et al. 1990, Menten et al. 1990, Menten & Melnick 1991, and Yates et al. 1995). Models for these maser lines predict that they are inverted more or less in the same shells of the envelope than the 22 GHz masers. There are also water vapor maser lines arising from the first vibrationally excited state of water $\nu_2=1$ (the bending mode): $4_{4,0}-5_{3,3}$ (96 GHz), $5_{5,0}-6_{4,3}$ (233 GHz), and $1_{1,0}-1_{0,1}$ (685 GHz), see Menten & Melnick (1989), and Menten & Young (1995). Since the excitation of these masers is much higher, it is assumed that they are originated in much more inner regions, like in the case of SiO masers (see Sect. 3.3).

The inversion mechanism of the ground state water masers is well understood. The upper level of the maser transitions always lie along (or near) the *backbone* (levels with $J_{1,J}$ or $J_{0,J}$ quantum numbers). Radiative transitions between levels along the backbone are very strong, and become optically thick at lower densities/column densities. Because of these high opacities, the collisional excitation of the H_2O molecules results in higher populations for backbone levels, leading to inversions w.r.t. levels somewhat lower in energy but away from the backbone (see e.g. Neufeld & Melnick 1991). For explaining the pumping/inversion of the vibrationally excited masers there is no satisfactory model yet (Alcolea & Menten 1993).

VLA observations of 22 GHz water masers (see e.g. Bowers & Johnston 1994, and Colomer et al. 2000), show that they arise from regions of the CEs with sizes of the order of 10^{15} cm, at distances to the central stars up to about 10 stellar radii. These works, although were unable to resolve the individual spots, indicate that in these regions of the envelope the gas is radially expanding but it has not yet reached the terminal velocity, i.e. the gas and dust are still being accelerated by the radiation pressure.

These results have been greatly improved by the works carried out with MERLIN which, thanks to its improved spatial resolution over the VLA, is able to resolve the individual maser spots, allowing a much better study of the water masers and the circumstellar shells from which they arise. Yates & Cohen (1994) identified the first proper motions of water masers, and also demonstrated that the size of the emitting region increases with the mass loss rate, as predicted by the models of Cooke & Elitzur (1985). These proper motions have been measured now in a number of objects: NML Cyg (Richards et al. 1996), VY CMa (Richards et al. 1998), S Per (Marvel 1996), and VX Sgr (Murakawa et al. 2003, Marvel 1996), all these four stars being super-giants. The results from the proper motion studies of the 22 GHz line are very consistent. The thin shell model which expands at constant velocity does not apply here. On the contrary, water vapor masers arise from a thick shell, some times not spherically symmetric. This shell is in radial expansion, but with a velocity that increases by a factor about two between the inner and outer limits of the maser region. This implies values of ϵ , the logarithmic velocity gradient, between 0.5 and 1.0.

Bains et al. (2003a) have recently published MERLIN observations of water masers in other types of AGB sources: the Mira variables U Her, U Ori and IK Tau, and the semi-regular variable RT Vir. Although in this case no proper motions are available, the velocity vs. position plots show that also in these cases, the radial velocity field has a clear outward gradient. It seems then that all these observations are given us information on the kinematics of the envelope when there is still some physics on it (other than free expansion). In fact, today there is no other way in which we can directly probe the velocity field in these regions of the envelope. In addition, when the (multi-epoch) observations include proper motion measurements, estimations for the distance to the star can be done assuming a simple structure for both the envelope and its velocity field. The results of these values for the distance are in fact in good agreement with those derived using other methods.

Very briefly, I would like not to forget the works by Imai et al. (2002 and 2004). These authors have also computed proper motions of the H₂O maser spots in circumstellar envelopes but of two early post-AGB stars, showing that in these cases water masers trace very young molecular bipolar outflows, that characterize this type of sources (see Sect. 4.).

3.3. Multi-transitional studies of circumstellar SiO masers

Circumstellar SiO masers are detected in the three main isotopic substitutions of SiO, ²⁸SiO, ²⁹SiO, and ³⁰SiO, in rotational transitions from the $J=1-0$ (at 43 GHz) up to the $J=8-7$ at (350 GHz) of the fundamental $v=0$ and $v=1$ to 4 vibrational excited states. SiO masers are located in the innermost layers of the circumstellar envelopes. This was soon suggested simply because of their high excitation requirements (the $v=1$ states of SiO are 1770 K above the $v=0$), from the shape of their spectra, and the fact that no large abundances of SiO are expected in the layers outside the dust formation layer. (The silicate dust grains in O-rich stars are in fact made of gaseous SiO after nucleation and condensation). However the exact location of the SiO maser remained unknown until the first VLBI true maps of the $v=1$ $J=1-0$ line showed that they consisted in a chain of spots delineating a ring of just a few stellar radii in diameter (Diamond et al. 1994). Although the position of the star in the map is not known (and this is still the case for all VLBI maps of SiO masers), the ring geometry strongly supports that the star should be located near the centroid of such structure.

The basic principle for explaining the inversion of SiO masers (for vibrationally excited transitions only) is very simple. It was proposed by Kwan & Scoville (1974), and it is based on the *self-trapping* phenomenon. For a SiO molecule in a vibrationally excited estate, the main de-excitation route is the decay, via ro-vibrational transitions, to lower vibrationally excited levels. When these transitions are optically thick, the escape probability of these photons is inversely proportional to the opacity of the line, and hence to the J quantum number of the upper state. Because of this, the higher the J value the less probable for a molecule to de-excite, resulting in a chain of inverted populations along the rotational ladder. Of course,

this mechanism only works provided that the inverted levels are populated at similar rates, i.e. not depending on the J number. This general inversion mechanism can be strongly modified by overlaps between the ro-vibrational lines of the SiO species and of other abundant molecules like H₂O (see e.g. Olofsson et al. 1981, and González-Alfonso & Cernicharo 1997).

As for the source of energy responsible for the pumping of the masers, there is still a debate after more than 30 yr since the discovery of these masers, and almost 14 yr since their first successful VLBI observations (Colomer et al. 1992). There are two main types of pumping mechanisms, termed *radiative* or *collisional* depending on the main source of energy responsible for the pumping. In collisional models, see e.g. Gray & Humphreys (2000) and Humphreys et al. (2002), the SiO molecules are pumped to $v \geq 1$ states via collisions with H₂, whereas in radiative models, see e.g. Bujarrabal (1994a and 1994b), the energy is obtained directly from the stellar 8 μ m IR radiation (the wavelength of the SiO $v=1-0$, 2-1, etc. ro-vibrational transitions).

Both models have pros and cons. On the one hand, for the radiative model to work, it is required that the absorption of the 8 μ m radiation is done under optically thin conditions, but I have just said that to attain the inversion these radiative de-excitations need to be optically thick. This situation is not contradictory if the SiO maser region presents a long velocity gradient, or has a thin shell geometry. Radiative models predict that SiO masers should show preferentially tangential amplification, i.e. the observed ring shapes, and that their intensity should vary in phase with the IR flux of the star, as it has also been observed (Alcolea et al. 1999, Pardo et al. 2004). On the other hand, collisional models do not need any especial geometry or velocity field for producing the population inversion, but they do need them for explaining the observed ring like distributions. However, the main drawback of these collisional models is that it is very difficult to explain how the maximum flux of all maser spots (including different maser transitions) occurs within less than one month. For example, for a maser ring thickness of $4.5 \cdot 10^{13}$ cm (i.e. 3 AU, or 6 m.a.s. at a distance of 500 pc, see Fig. 1), we need a physical process traveling at speeds larger than 90 km s⁻¹ to affect all the maser spots in less than 60 days.

The observation of a single SiO maser line does not help very much in supporting one model against the other, since both can predict the observed source size and maser strength. However, it is expected that the observations of several lines, with similar and different excitations, impose more severe constraints to the models, helping in determining which is the correct (if any). These multi-transitional observations need to be (almost) simultaneous, since SiO masers vary both in intensity and location in the shell (Diamond & Kemball 2003). During the last century, VLBI observations of SiO masers concentrated on a single line, the $v=1$ $J=1-0$ of ²⁸SiO in their majority, but in the past few years simultaneous observations of two, three, and up to four ²⁸SiO maser lines have become available.

The comparisons of the distributions of the $v=1$ and $v=2$ $J=1-0$ masers have reached, I think, a firmly established result. As it was first pointed out by Desmurs et al. (2000), both masers show distributions which are very much alike. It is true

that both transitions share some emitting regions, but for the majority of the spots there is a systematic shift of about 1 m.a.s. between the two maser lines, the spots of the $v=1$ being always farther away. This result holds regardless of the optical phase of the star (Cotton et al. 2004). Such a small difference seems very surprising for two lines so separated in excitation (1770 vs. 3540 K) and this is very difficult to explain using the standard models for SiO masers. This problem becomes even more severe when considering also the comparison between the $v=1$ $J=2-1$ and $J=1-0$ masers. So far we have only data of such a comparison for three sources, but the results are shocking. In the case of IRC +10011, Soria-Ruiz et al. (2004a and 2004b, see also Fig. 1) have obtained for two epochs that, in spite of being two adjacent transitions, the differences between the two $v=1$ lines are much larger, 4 m.a.s., than those for the two $J=1-0$ lines (which, as I mentioned before, are 1770 K apart). From inside to outside they find the rings of the $v=2$ $J=1-0$ line, then the $v=1$ $J=1-0$, and finally the $v=1$ $J=2-1$. The same series of rings have also been found by Winter et al. (2002) in R Cas in three different epochs. (A fourth epoch of R Cas has been published by Phillips et al. 2003, but since these authors did not map the $v=2$ $J=1-0$, we can not examine whether the $v=1$ $J=1-0$ is more like the $v=2$ or like the $v=1$ $J=2-1$.)

As pointed out by Soria-Ruiz et al. (2004a), these results are incompatible with current pumping models for SiO masers, since all predict very similar spatial distributions for lines within the same vibrational state, and different ones for lines with very different excitation. These authors propose that the line overlap between ro-vibrational transitions of H₂O and SiO may solve the problem. In fact they conclude that, by introducing the effects of the extra opacity in the $v=2-1$ $J=1-0$ ro-vibrational transition of ²⁸SiO due to the $v_2=1-0$ 11_{6.6}-12_{7.5} of H₂O, the distribution of the masers in IRC +10011 can be explained (see also Bujarrabal et al. 1996).

This hypothesis is also supported by the results obtained for χ Cyg, where Soria-Ruiz et al. (2004a) also detected the $v=2$ $J=2-1$ maser. In this case the two $v=1$ masers delineate rings of about the same size, whereas both $v=2$ masers are much more compact, just as expected from classical pumping models. However χ Cyg is a S-type star, for which H₂O abundances lower than those in O-rich sources (like IRC +10011 and R Cas) are expected. In fact, neither H₂O nor OH masers have been detected in this source (Benson et al. 1990), and therefore it seems very probable that the effects of the proposed overlap could be much weaker here.

These are of course very preliminary results, that need much further investigation (both from the observational and theoretical point of view), but my understanding is that from now on we should face the fact that for modeling SiO masers in circumstellar envelopes, the effects of the line overlaps can not be neglected. I must also note this *anomalous* shift between the $v=1$ $J=1-0$ and $J=2-1$ masers of ²⁸SiO has also been reported by Doeleman et al. (2004) in Ori A Irc 2.

4. Rotation and magnetic fields in post-AGB envelopes and before

As I said before, at the end of the AGB, the *super-wind* phase, the mass loss rate can be as large as $10^{-4} M_{\odot} \text{ yr}^{-1}$. Obviously, the star can not endure such an enormous mass loss rate for a long time. After a few ten thousand years the H/He-burning shells become literally exposed, and the star turns extremely hot and tiny becoming a blue dwarf. This transformation occurs very rapidly, lasting no more than a few thousand years. Meanwhile, the circumstellar envelope is deeply changed. The heavy mass loss has stopped, and the CE becomes thinner and thinner as it keeps expanding, being first photo-dissociated and then photo-ionized by the hard UV radiation emanating from the hot central star (once it becomes hotter than 30,000 K), leading to the formation of a Planetary Nebula (PN). The shaping of the PN is also due to the interaction of the slow wind from the AGB phase (the former CE) with a more tenuous, but faster and hotter one, that is released by the central star at this stage. This Interacting Stellar Wind (ISW) model was proposed by Kwok et al. (1978) to explain the morphology of spherical PNe. However, this interaction can only produce spherically symmetric PN. Nowadays there is mounting evidence that in general PNe are anything but spherical, and therefore modifications to the ISW model are required.

Traditionally for explaining non-spherically symmetric PNe it has been assumed that during the super-wind phase, at the end of the AGB, the mass loss is not isotropic but somehow enhanced along certain equatorial plane. The interaction of this non-isotropic AGB wind with the isotropic wind in the PN phase would naturally result in the formation of asymmetric PNe: this modification of the ISW model is known as the GISW (Generalized ISW) model (Mellema & Frank 1995). However there is a major problem: in general, AGB envelopes have little deviation from the spherical symmetry, as one would expect for an isotropic loose of mass. This has been proved by means of observations of the CO emission (Neri et al. 1998), OH and SiO masers (see previous sections), and the detection of concentric rings/arcs of dust scattered light around AGB and post-AGB sources (see Balick & Frank 2002).

Today we know that the shaping of these asymmetrical PNe is probably due to the interaction of a fast collimated wind, released at the very end of the AGB phase, which collides with the slow moving AGB wind. These bipolar flows are observed by means of high velocity emission in molecular and atomic lines of post-AGB stars, whose envelopes have not yet attain the PN phase, the so called pre-PNe (PPNe). About what powers these jets the only thing we know is that radiation pressure is not responsible for them (Bujarrabal et al. 2001, see also Alcolea 2004 for a review on the characteristics of these bipolar ejecta, and their importance in the shaping of PPNe and PNe). Not having other candidates, and based also in the universal connection between bipolar flows and rotating strong magnetic fields (AGNs, micro- and nano-quasars, proto-stars, pulsars), some authors have postulated that a process similar to the magneto-centrifugal mechanism may operate in late AGB and post-AGB sources.

The best way of having a look at any possible rotation in CEs using VLBI is to observe SiO masers. Since they are the closest to the star, it is expected that they show larger rotation velocities. So far, the detection of rotation from VLBI observations of SiO masers has been claimed only in four stars. Hollis et al. (2001) have found that the SiO masers in R Aqr are in almost Keplerian rotation. However, this case is somewhat special since it is a well known symbiotic system displaying a hourglass nebula. Sánchez-Contreras et al. (2002) also found that positions and velocities of the SiO maser spots in OH 231.8+4.1 could indicate rotation. Again OH 231.8+4.2 is not a normal example since it is highly bipolar post-AGB source (see Alcolea et al. 2001). Boboltz & Marvel (2000) also reported rotation from the SiO masers in the supergiant NML Cyg. However they assumed a systemic velocity of -6.6 km s^{-1} , whereas from thermal CO emission the systemic velocity is about -1 km s^{-1} (Kemper et al. 2003). Cotton et al. (2004) reported indications of rotation just in R Aqr and possibly in S CrB, out of the nine targets observed. In summary, excluding *peculiar* cases, of about a dozen stars mapped in SiO maser emission, there may be indications of rotation only in two of them. Therefore, it seems that rapid rotation is not a common feature to AGB stars, but further investigation is required.

Polarization measurements of the different masers can tell us about the strength of the magnetic field in circumstellar envelopes. SiO masers usually show linear polarization tangential to the circles they delineate, i.e. perpendicular to the radial direction (see e.g. Kemball & Diamond 1997, and Desmurs et al. 2000). However, this is a natural result if the masers are pumped via the stellar radiation (since the linear polarization vector must be orthogonal to both the direction of the amplification of the masers and of the pumping radiation). Circular polarization of SiO masers is less frequently observed. Kemball & Diamond (1997) reported its detection in TX Cam, implying (according to these authors) magnetic fields of 5–10 G for the SiO maser region. The situation is more clear for OH and H₂O masers. The works on OH masers by Szymczak & Gérard (2004) and Bains et al. (2003b and 2004) are systematically finding polarization properties consistent with magnetic fields of the order of a few mG. The studied sources are always PPNe or candidates to be PPNe, and in some cases it seems that the non spherical symmetry of the nebula could be related to the structure of the magnetic field (see also Etoka & Diamond 2004, and Szymczak et al. 2001). Very recently Vlemmings et al. (2002) have measured the circular polarization of the H₂O masers in three super-giants, NML Cyg, VY CMa, and S Per, and the Mira variable U Her. The values obtained for the magnetic field are 100–500 mG for the super-giants and about 1 G for the Mira variable. As we see the data are still scarce, but I think that the potential of polarization measurements in probing the magnetic field in AGB and post-AGB stars is clear, and that these type of works will provide useful constrains for models of bipolar flow launching at these stages of the stellar evolution.

5. A look into the future

Just from the few examples I just presented, I think that we can conclude that the VLBI observations of circumstellar maser lines are providing wonderful results with great impact not only on the maser phenomenon itself and the physical and chemical processes of AGB envelopes, but also on other basic fields in Astronomy (such as the Astrometry of stars with its implications on the dynamics and stellar population of the Galaxy). However, with the use of the new instrumentation that is now becoming available, or will become available in the next coming years, it is easy to foresee an even more brilliant future for VLBI circumstellar maser research.

The already operating networks of the HSA and GMVA will lower the detection limit, especially in the 3 mm band, allowing a much better study of weak maser lines, such as $v=3$ $J=1-0$ ²⁸SiO masers or the HCN masers at 89 GHz. The new 40 m dish now being built in Yebes will certainly join these networks soon, helping in solving the collecting area limitation of VLBI at mm wavelengths. Also, the EVLA plus the VLBA will be a perfect instrumental combination for observing $J=1-0$ SiO masers at 43 GHz, as it is the EVN plus MERLIN at lower frequencies.

In principle, the development of *e*EVN does not represent a sensitivity improvement over the traditional way of VLBI observing. However it will certainly offer an opportunity for easing the planning and scheduling of the observing sessions. In particular, having more than three EVN sessions per year will greatly improve the reliability of proper motion measurements against the *Christmas Tree* effect. Note that for the case of maser lines, relatively narrow bands (as compared with continuum observations) are needed. Therefore, setting up an *e*EVN network for line studies does not require so much networking bandwidth, being much cheaper to operate.

The Japanese VERA project will represent a major breakthrough for circumstellar maser studies. This will be a dedicated phase reference array to measure annual parallax and proper motions of AGB stars, observing their masers at 22 GHz (H₂O) and 43 GHz (SiO). In addition to provide positions to an accuracy of 10 μas ., and precise distances anywhere in the Galaxy, the project will also release maps of these two maser lines in a large number of sources.

The Observatorio Astronómico Nacional (OAN) is engaged in the ALMA project, that at its highest operative frequencies will provide spatial resolutions up to 6 m.a.s. Its enormous collecting area will let us accurately map many spectral lines in circumstellar envelopes, as well as to locate the central star. It is possible that combining ALMA and VLBI observations of SiO masers at 3 mm we could finally place the star at the center of the maser rings.

Moving higher in frequencies, it is planned that the Herschel satellite will fly sometime in 2007. One of the major tasks for the heterodyne instrument on board, HIFI (in which the OAN is deeply involved too), will certainly be the exploration of water lines everywhere. In this context, circumstellar envelopes offer a unique opportunity because of their simple geometry and kinematics, and the wide range of physical conditions they exhibit. This instrument however, will be unable to

resolve the emission from water in CEs, the analysis of the results being largely dependent on their modeling. Here is where a good knowledge of the different CE regimes, via interferometric/VLBI observations of all OH, H₂O and SiO maser lines, may play a key role.

Going even higher in frequencies, the two interferometric instruments at the VLTI, VLTI-VINCI (near-IR) and VLTI-MIDI (mid-IR), will offer a unique opportunity to study the inner parts of CEs. VLTI-VINCI is able to measure the size of the central star and monitor its changes in size and temperature along the pulsation cycle. VLTI-MIDI will do a similar work but for the dust formation layer. It is clear that the combination of these two instruments with VLBI observations of SiO and 22 GHz water masers, will give us a superb picture of the central star and its influence through the SiO-maser and water-maser/dust-formation layers (see e.g. Wittkowski & Boboltz 2003).

And of course, we should not forget the SKA project, that will certainly change the way we think about VLBI.

Acknowledgements. This contribution would not have been possible without the help of the VLBI group at the OAN. I appreciate very much J.-F. Desmurs and R. Soria-Ruiz for their critical reading of the manuscript, and the editors of this proceedings book for their patience. I also want to thank my wife for her comprehension, and my kids for making such a joyful noise around, during the writing of this contribution. This work has been financially supported by the Spanish DGI (MCYT) under projects AYA2000-0927 and AYA2003-7584, and by the European Commission's I3 Programme "RADIONET", under contract No. 505818.

References

Alcolea, J., 2004, in Springer Proceedings in Physics 91, The Dense Interstellar Medium in Galaxies, ed. S. Pfalzner, C. Kramer, C. Staubmeir, A. Heithausen, 593

Alcolea, J., Bujarrabal, V., Sánchez Contreras, C., Neri, R., Zweigle, J., 2001, A&A 373, 932

Alcolea, J., Menten, K. M., 1993, in Lecture Notes in Physics 412, Astrophysical masers, ed. A. W. Clegg, G. E. Nedoluha, 399

Alcolea, J., Pardo, J. R., Bujarrabal, V., et al., 1999, A&AS 139, 461

Bains, I., Cohen, R. J., Louridas, A., et al., 2003a, MNRAS 342, 8

Bains, I., Gledhill, T. M., Yates, J. A., Richards, A. M. S., 2003b, MNRAS 338, 287

Bains, I., Richards, A. M. S., Gledhill, T. M., Yates, J. A., 2004, MNRAS (in press)

Balick, B., Frank, A., 2002, ARA&A 40, 439

Baud, B., 1981, ApJ 250, L9

Benson, P. J., Little-Marenin, I. R., Woods, T. C., et al., 1990, ApJS 74, 911

Boboltz, D. A., Marvel, K. B., 2000, ApJ 545, L149

Booth, R. S., Kus, A. J., Norris, R., Porter, N. D., 1981, Nature 290, 382

Bowers, P. F., Johnston, K. J., 1994, ApJS 92, 189

Bujarrabal, V., 1994b, A&A 285, 953

Bujarrabal, V., 1994b, A&A 285, 971

Bujarrabal, V., Alcolea, J., Sánchez Contreras, C., Colomer, F., 1996, A&A 314, 883

Bujarrabal, V., Castro-Carrizo, A., Alcolea, J., Sánchez Contreras, C., 2001, A&A 377, 868

Cernicharo, J., Thum, C., Hein, H., et al., 1990, A&A 231, L15

Colomer, F., Graham, D. A., Krichbaum, T. P., et al., 1992, A&A 254, L17

Colomer, F., Reid, M. J., Menten, K. M., Bujarrabal, V., 2000, A&A 355, 979

Cooke, B., Elitzur, M., 1985, ApJ 295, 175

Cotton, W. D., Mennesson, B., Diamond, P. J., et al., 2004, A&A 414, 275

Desmurs, J.-F., Bujarrabal, V., Colomer, F., Alcolea, J., 2000, A&A 360, 189

Diamond, P. J., Kemball, A. J., Junor, W., et al., 1994, ApJ 430, L61

Diamond, P. J., Kemball, A. J., 2003, ApJ 599, 1372

Doeleman, S. S., Lonsdale, C. J., Kondratko, P. T., Predmore, C. R., 2004, ApJ 607, 361

Etoka, S., Diamond, P., 2004, MNRAS 348, 34

González-Alfonso, E., Cernicharo, J., 1997, A&A 322, 938

Gray, M. D., Humphreys, E. M. L., 2000, New Astron. 5, 155

Habing, H. J., 1996, A&ARv 7, 97

Herman, J., Habing, H. J., 1985, A&AS 59, 523

Hollis, J. M., Boboltz, D. A., Pedelty, J. A., White, S. M., Forster, J. R., 2001, ApJ 559, L37

Humphreys, E. M. L., Gray, M. D., Yates, J. A., et al., 2002, A&A 386, 256

Imai, H., Morris, M., Sahai, R., Hachisuka, K., Azzollini, F., J. R., 2004, A&A 420, 265

Imai, H., Obara, K., Diamond, P. J., Omodaka, T., Sasao, T., 2002, Nature 417, 829

Izumiura, H., Ukita, N., Tsuji, T., 1995, ApJ 440, 728

Jewell, P. R., Webber, J. C., Snyder, L. E., 1980, ApJ 242, L29

Kemball, A. J., Diamond, P. J., 1997, ApJ 481, L111

Kemper, F., Stark, R., Justtanont, K., et al., 2003, A&A 407, 609

Kwan, J., Scoville, N., 1974, ApJ 194, L97

Kwok, S., Purton, C. R., Fitzgerald, P. M., 1978, ApJ 219, L125

Lipman, E. A., Hale, D. D. S., Monnier, J. D., et al., 2000, ApJ 532, 467

Lucas, R., Cernicharo, J., 1989, A&A 218, L20

Lucas, R., Omont, A., Guilloteau, S., 1988, A&A 194, 230

Marvel, K. B., 1996, PhD thesis, New Mexico State Univ.

Mellema, G., Frank, A., 1995, MNRAS 273, 401

Menten, K. M., Melnick, G. J., 1989, ApJ 342, L91

Menten, K. M., Melnick, G. J., 1991, ApJ 377, 647

Menten, K. M., Melnick, G. J., Phillips, T. G., 1990, ApJ 350, L41

Menten, K. M., Young, K., 1995, ApJ 450, L67

Murakawa, K., Yates, J. A., Richards, A. M. S., Cohen, R. J., 2003, MNRAS 344, 1

Neri, R., Kahane, C., Lucas, R., Bujarrabal, V., Loup, C., 1998, A&AS 130, 1

Neufeld, D. A., Melnick, G. J., 1991, ApJ 368, 215

Nguyen-Q-Rieu, Bujarrabal, V., Olofsson, H., Johansson, L. E. B., Turner, B. E., 1984, ApJ 286, 276

Olofsson, H., 1999, in Asymptotic Giant Branch Stars, IAU Symposium 191, ed. T. Le Bertre, A. Lebre, C. Waelkens, 30

Olofsson, H., Rydbeck, O. E. H., Lane, A. P., Predmore, C. R., 1981, ApJ 247, L81

Pardo, J. R., Alcolea, J., Bujarrabal, V., et al., 2004, A&A 424, 145

Phillips, R. B., Straughn, A. H., Doeleman, S. S., Lonsdale, C. J., 2003, ApJ 588, L10

Richards, A. M. S., Yates, J. A., Cohen, R. J., 1996, MNRAS 282, 665

Richards, A. M. S., Yates, J. A., Cohen, R. J., 1998, MNRAS 299, 319

Sánchez Contreras, C., Desmurs, J.-F., Bujarrabal, V., Alcolea, J., Colomer, F., 2002, A&A 385, L1

Schilke, P., Mehringer, D. M., Menten, K. M., 2000, ApJ 528, L37

Schilke, P., Menten, K. M., 2003, ApJ 583, 446

Soria-Ruiz, R., Alcolea, J., Colomer, F., et al., 2004a, A&A in press

Soria-Ruiz, R., Colomer, F., Alcolea, J., et al., 2004b, this proceedings

Spaans, M., van Langevelde, H. J., 1992, MNRAS 258, 159

Szymczak, M., Cohen, R. J., Richards, A. M. S., 2001, A&A 371, 1012

Szymczak, M., Gérard, E., 2004, A&A 423, 209

Vinkovic, D., Blöcker, T., Hofmann, K.-H., Elitzur, M., Weigelt, G., 2004, MNRAS 352, 852

Vlemmings, W. H. T., Diamond, P. J., van Langevelde, H. J., 2002, A&A 394, 589

Vlemmings, W. H. T., van Langevelde, H. J., Diamond, P. J., Habing, H. J., Schilizzi, R. T., 2003, A&A 407, 213

Winter, L. M., Phillips, R. B., Crowley, R. J., 2002, 201st AAS Meeting, Bulletin of the AAS 34, 1291

Wittkowski, M., Boboltz, D. A., 2003, in ASP Conference Series (in press), Future Directions in High Resolution Astronomy: The 10th Anniversary of the VLBA, ed. J. D. Romney, M. J. Reid

Yates, J. A., Cohen, R. J., 1994, MNRAS 270, 958

Yates, J. A., Cohen, R. J., Hills, R. E., 1995, MNRAS 273, 529

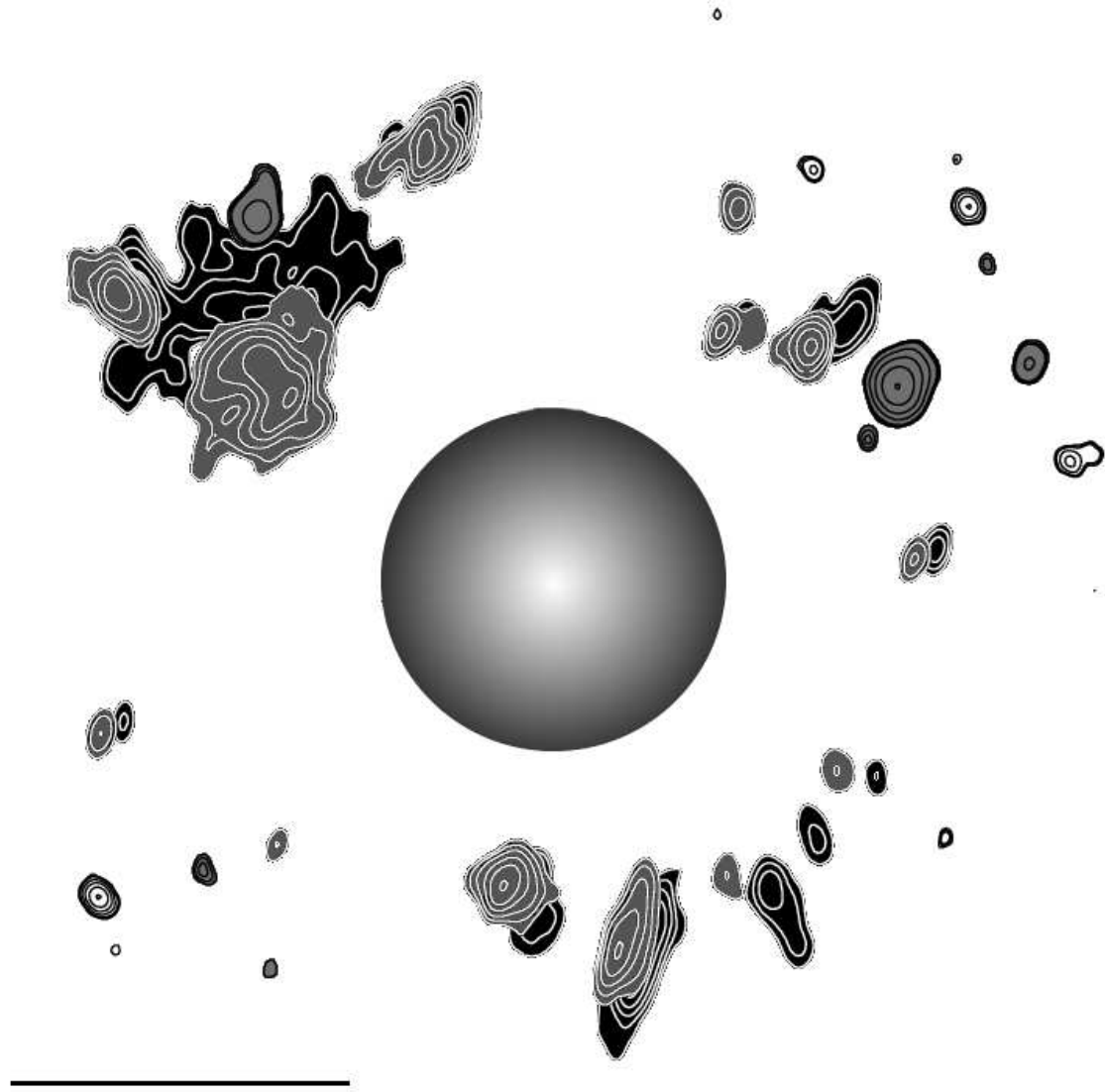


Fig. 1. Distribution of SiO masers in the innermost shells of the circumstellar envelope around the long period variable IRC+10011 after Soria-Ruiz et al. (2004b). These authors observed four different maser lines, $^{28}\text{SiO } v=1 J=1-0$ (black with white contours), $^{28}\text{SiO } v=2 J=1-0$ (grey with white contours), $^{28}\text{SiO } v=1 J=2-1$ (white with black contours), and $^{29}\text{SiO } v=0 J=1-0$ (grey with black contours), with excitation temperatures from zero to more than 3500 K. To relatively align the different maps, the centroids of all the transitions have been assumed to be at the center of the star. The diameter of the star, 11 m.a.s., is taken from the model by Vinkovic et al. (2004). The horizontal black line has a length of 10 m.a.s. in the scale of the plot (which translates into a linear size of $7.3 \cdot 10^{13}$ cm for a distance to the source of 500 pc). The maser spots clearly delineate a ring, approximately located between 1 and 2 stellar radii. In this object, it has been measured that the first layers of thick dust are located at a radius of 33 m.a.s., about 6 stellar radii (Lipman et al. 2000).

This figure "JAlcolea-fig1.png" is available in "png" format from:

<http://arxiv.org/ps/astro-ph/0412295v1>